

# X-ray fluorescence attachment for rapid in-house evaluation of heavy atom derivative crystals in protein crystallography and in-house MAD using the dual wavelength system

Takashi Matsumoto\*, Kimiko Hasegawa\*\* and Tomokazu Hasegawa\*\*\*

## 1. Introduction

Structural information of a protein molecule is very important for investigating protein function. MAD phasing continues to play a crucial role in the structure determination of novel proteins. In addition, the conventional method of heavy atom derivatization for the purpose of phasing still plays a crucial role in protein crystallography in novel protein structure determination. Here, we introduce a product that improves the efficiency of protein structure determination using an X-ray fluorescence attachment and a dual wavelength X-ray system.

## 2. Evaluating the presence of heavy atoms in crystals using X-ray fluorescence

### 2.1. Introduction

The standard methods for determination of novel protein crystal structures include multiple and single isomorphous replacement (MIR and SIR), multiple and single isomorphous replacement with anomalous scattering (MIRAS and SIRAS) and multi and single wavelength anomalous dispersion (MAD and SAD). To be successful, these methods require a high occupancy of heavy atoms sites bound to the protein in the crystals. To acquire adequate heavy atom derivative crystals, soaking experiments are carried out by transferring a large number of well diffracting crystals to numerous heavy atom solutions for minutes to days<sup>(1)</sup>. Moreover, the evaluation of derivatization requires calculating a difference Patterson map from a full data collection. Therefore, the preparation of heavy atom derivatives is a trial and error process that may require much iteration. The fact that diffraction data must be collected to determine whether a heavy atom derivative has been formed means that this is a long and tedious process. If the presence of heavy atoms in a protein crystal can be determined prior to a data collection the amount of work required to obtain heavy atom derivatives would be greatly reduced.

X-ray fluorescence (XRF) is the emission of characteristic secondary X-ray from a sample that has

been excited by irradiating with high energy X-rays. XRF provides elemental composition of an irradiated sample. The intensity an XRF spectrum is related to the relative amount of each element and thus XRF has a potential for screening protein crystals to determine is heavy atoms have incorporated into the crystal lattice. We have developed an XRF attachment that is used to detect heavy atoms introduced by soaking. This XRF attachment is composed of a silicon drift detector (SDD), a stage, counting circuits and software, and can be added to an existing in-house single crystal system.

To validate this system, we soaked protein crystals in heavy atom solutions and performed both XRF and X-ray diffraction (XRD) measurements.

### 2.2. Sample preparation

The crystals of hen egg-white lysozyme (Sigma, 20 mg ml<sup>-1</sup> in 50 mM sodium acetate pH 4.7) were grown by vapour diffusion at 20°C using a reservoir solution of 6% PEG8000, 15% NaCl and 50 mM sodium acetate pH 4.7.

The lysozyme soaking experiments were carried out by transferring native crystals to a platinum solution containing 6% PEG8000, 15% NaCl and 50 mM sodium acetate pH 4.7 supplemented with 2 mM K<sub>2</sub>PtCl<sub>4</sub>, 4 mM K<sub>2</sub>PtCl<sub>4</sub>, 10 mM K<sub>2</sub>PtCl<sub>4</sub>. The lysozyme crystals were soaked in a 2 mM K<sub>2</sub>PtCl<sub>4</sub> solution for 130 min, designated hereafter as (I). Other derivatives were prepared using different soaking conditions: (II) and (III), (IV).

After soaking, putative lysozyme derivative crystals were transferred into a cryoprotectant solution (10% Glycerol, 6% PEG8000, 15% NaCl and 50 mM sodium acetate pH 4.7) and frozen by plunging into liquid nitrogen.

### 2.3. Evaluation of the presence of heavy atoms in crystals using X-ray fluorescence and X-ray diffraction

This XRF attachment was placed on a MicroMax007HF rotating anode X-ray generator equipped with a VariMax multilayer optic.

The XRF signal was measured with the XRF attachment with the protein crystals cooled to 93 K.

The XRF spectra were measured for crystals from

\* Application Laboratories, Rigaku Corporation.

\*\* Global Marketing Group, Rigaku Corporation.

\*\*\* SBU Single Crystal Group, Rigaku Corporation.

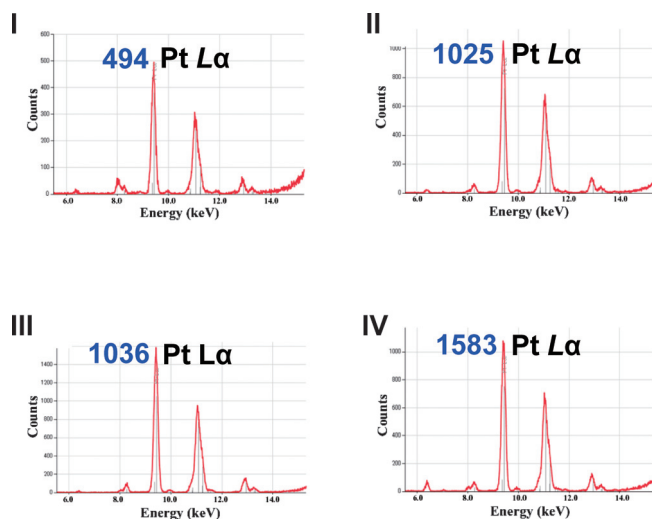


**Fig. 1.** XRF spectra from each derivative (accumulation time: 300 seconds).

I: 2 mM  $K_2PtCl_4$  130 min soaking

II: 2 mM  $K_2PtCl_4$  63 hr soaking

III: 4 mM  $K_2PtCl_4$  450 min soaking

IV: 10 mM  $K_2PtCl_4$  10 min soaking

\*The numbers shown in blue in Fig. 1 and Table 1 indicate total measured counts for the Pt  $L\alpha$  line.

four different soaking conditions (I, II, III and IV) using the XRF attachment. The two major XRF peaks from each crystal were measured for 300 seconds (Fig. 1).

The two large peaks are the emission lines of Pt  $L\alpha$  and  $L\beta$  fluorescence, respectively. Comparison of the spectra indicates that the platinum  $L\alpha$  signal increases proportional to both the total number and occupancy of incorporated platinum atoms. To confirm whether the heavy atoms actually bind to protein, we collected diffraction data sets using a MicroMax007HF rotating anode generator equipped with a Saturn 724<sup>+</sup> CCD detector.

The heavy atom binding sites were identified from the Difference Fourier ( $F_{PH}-F_P$ ) maps (Fig. 2). The lower XRF signal resulted in lower heavy atom peak heights and fewer heavy atom sites (Fig. 2 and Table 1). In spite of similar XRF signal counts for II and III, these derivatives clearly showed different characteristics. Sample III had one significantly higher occupancy site and a few low occupancy sites. On the other hand, sample II had many low occupancy sites only. Moreover, one platinum binding site of sample III was clearly indicated in the anomalous difference Fourier ( $F_{PH}^+-F_{PH}^-$ ) map (Fig. 2 and Table 1). The XRF signal height was in proportion to the amount of heavy atoms incorporated into a protein crystal.

## 2.4. Results

The results of this test show that you can detect a trace amount of heavy atoms in a protein crystal introduced by soaking and therefore one can estimate the quality of heavy atom derivatives without data collection.

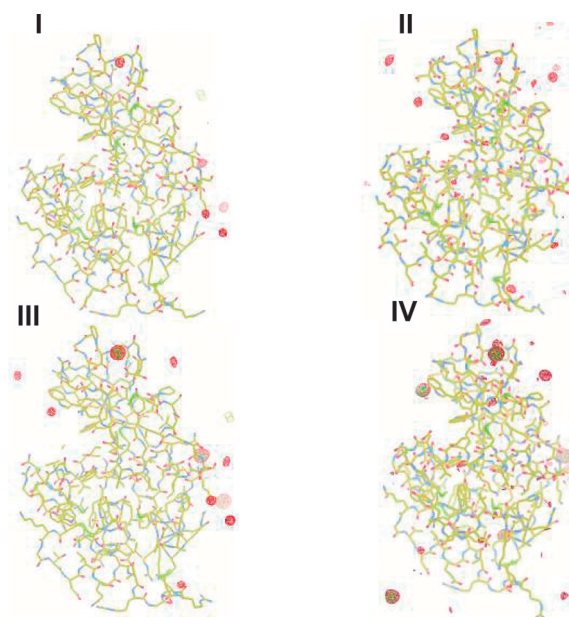


**Fig. 2.** Difference Fourier ( $F_{PH}-F_P$ ) map of bound heavy atom at  $3.5\sigma$  (red), and the anomalous different Fourier ( $F_{PH}^+-F_{PH}^-$ ) map from heavy atom at  $4.5\sigma$  (green).

\*In Table 1, the peak heights from difference Fourier maps and anomalous difference Fourier maps are shown in red and green respectively.

**Table 1.** Platinum  $L\alpha$  signal counts and difference Fourier peak heights.

Data set name	I	II	III	IV
X-ray fluorescence measurements				
Platinum $L\alpha$ signal counts	494	1025	1036	1583
Difference Fourier peak heights				
Site 1 ( $\sigma$ )	7.56	6.64	23.28	38.62
Site 2 ( $\sigma$ )	<5.0	<5.0	<5.0	16.85
Site 3 ( $\sigma$ )	6.47	5.12	7.69	<5.0
Site 4 ( $\sigma$ )	<5.0	8.71	7.75	<5.0
Site 5 ( $\sigma$ )	<5.0	8.01	5.97	6.42
Site 6 ( $\sigma$ )	<5.0	5.98	<5.0	<5.0
Site 7 ( $\sigma$ )	<5.0	5.85	<5.0	<5.0
Anomalous difference Fourier peak heights				
Site 1 ( $\sigma$ )	<5.0	<5.0	11.11	22.67
Site 2 ( $\sigma$ )	<5.0	<5.0	<5.0	9.41

The XRF attachment greatly simplifies soaking experiments by reducing the number of data collections that must be performed (Fig. 3). This is because one does not have to collect data when the XRF signal corresponding to intended heavy atoms is absent. This XRF tool also provides information on the amount of heavy atoms introduced into a protein crystal. A crystal having a significantly strong XRF signal probably is a

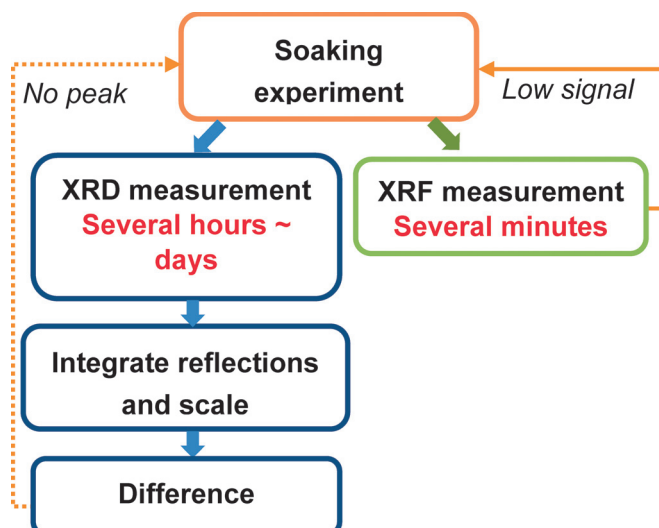


Fig. 3. The schematic drawing of heavy atom derivative search with or without XRF measurement.

good derivative.

### 3. Protein structure determination using MAD phasing with an in-house dual wavelength system

#### 3.1. Introduction

The multiple isomorphous replacement method (MIR) still plays a crucial role in structure determination of novel proteins. For the MIR technique to be successful the crystals of the different derivatives must be isomorphous with crystals of the native protein. However, the phasing power of heavy-atom derivatives is often compromised by the lack of isomorphism. The SAD technique requires a high occupancy of heavy atom derivatives. The MAD technique avoids these two problems by using multiple datasets at different wavelengths measured from a single crystal. MAD phasing is a very useful method for protein crystallography.

Recently, Rigaku's RAPID II curved imaging plate detector has been combined with a new dual-wavelength rotating anode X-ray generator. The MicroMax-007HF DW is equipped with a dual wavelength multilayer optics, VariMax DW, which allows easy switching between two wavelengths without moving the sample.

With this system it is easy to collect the data at two different wavelengths using an in-house system.

To validate this system, we soaked lysozyme crystals in a platinum complex solution and performed both  $MoK\alpha$  and  $CuK\alpha$  XRD measurements.

#### 3.2. Sample preparation

The lysozyme crystals were soaked in a 10mM  $K_2PtCl_4$  solution for 10 min. After soaking, lysozyme derivative crystals were transferred into a cryoprotectant solution (10% Glycerol, 6% PEG8000, 15% NaCl and 50mM sodium acetate pH 4.7) and frozen by plunging into liquid nitrogen.

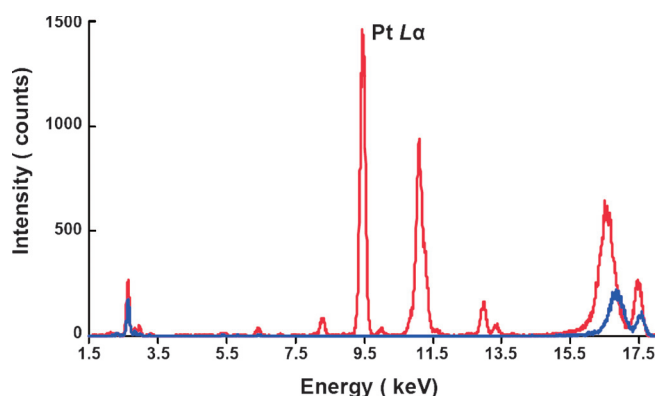


Fig. 4. XRF spectra from native and derivative crystals. (accumulation time: 300 seconds). Blue: Native crystal Red: Pt-derivative crystal.

#### 3.3. $MoK\alpha$ and $CuK\alpha$ measurements and MAD analysis

The XRF attachment was placed on a RAPID II diffractometer with a MicroMax-007HF DW generator and VariMax DW optics.

We checked heavy atom soaked lysozyme crystals with the XRF attachment using  $MoK\alpha$  radiation (Fig. 4). When we measured a significantly high XRF peak for Pt, we collected the data using Mo radiation, and then switched to Cu radiation for another data set (Table 2).

The MAD phase from the  $MoK\alpha$  and  $CuK\alpha$  data sets resulted in good electron density maps and was sufficient for auto model building using the program BUCCANEER<sup>(2)</sup> from the CCP4 program package<sup>(3)</sup>. Due to the low Pt occupancy of soaked lysozyme crystals, SIRAS and SAD phases resulted in electron density for which model building could not be performed (Table 3 and Fig. 5).

#### 3.4. Results

This XRF attachment works better when used with Mo radiation because of the higher energy compared

**Table 2.** Data collection and refinement statistics.

Sample name	Lysozyme	
Soaking condition	10 mM K <sub>2</sub> PtCl <sub>4</sub> 10 min	
	X-ray diffraction measurements	
Wavelength	CuK $\alpha$ ( $\lambda$ =1.54187 Å)	MoK $\alpha$ ( $\lambda$ =0.71075 Å)
Detector	RAPID II	
Space group	<i>P</i> <sub>4</sub> <sub>3</sub> <sub>2</sub> <sub>1</sub> <sub>2</sub>	<i>P</i> <sub>4</sub> <sub>3</sub> <sub>2</sub> <sub>1</sub> <sub>2</sub>
Unit cell (Å)	<i>a</i> =77.50 <i>b</i> =77.50 <i>c</i> =38.44	<i>a</i> =77.61 <i>b</i> =77.61 <i>c</i> =38.23
Resolution (Å)	27.40–1.40 (1.45–1.40)	12.93–1.80 (1.86–1.80)
Completeness (%)	100.0 (99.7)	99.9 (100.0)
<i>R</i> <sub>merge</sub> (%)	7.6 (43.5)	13.7 (60.7)
Figure of merit*	0.21	
	Refinement statistics	
Resolutions (Å)	27.40–1.40	
<i>R</i> factor (%)	18.61	
<i>R</i> <sub>free</sub> (%)	22.04	

\*Figure of merit:  $\langle |\sum P(\alpha)e^{i\alpha} / \sum P(\alpha)| \rangle$ , where  $\alpha$  is the phase and  $P(\alpha)$  is the phase probability distribution.

**Table 3.** Phase comparison.

	MAD	SIRAS (CuK $\alpha$ )	SIRAS (MoK $\alpha$ )	SAD (CuK $\alpha$ )	SAD (MoK $\alpha$ )
Resolution (Å)	27.40 –1.40	27.40 –1.40	12.93 –2.00	27.40 –1.40	12.93 –1.80
Figure of merit	0.21	0.18	0.09	0.18	0.17

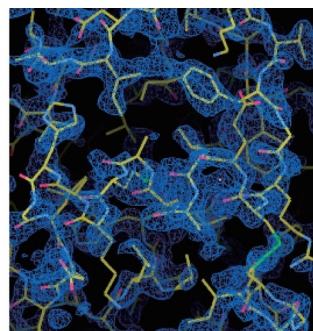
to Cu radiation. With the VariMax DW with RAPID II, one can check the heavy atom derivatives with the XRF attachment and collect the data using Mo radiation, and then switch to Cu radiation for data collection.

The combination of VariMax DW with RAPID II and the XRF attachment can greatly reduce the amount of work required to perform MAD/SAD/MIR/SIR phase determination by eliminating unnecessary data collections and by “RAPID” data collections for good derivatives.

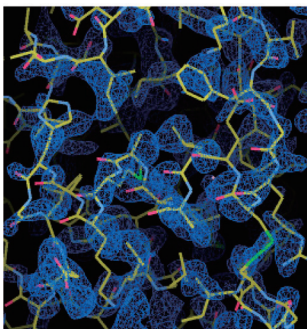
#### 4. Introduction of equipment

##### 4.1. Dual-wavelength system for single crystal structure analysis

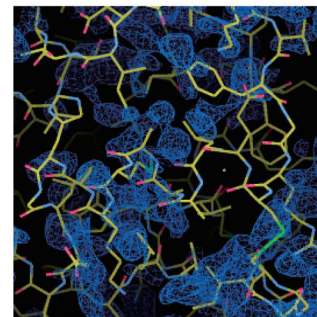
Rigaku has two different models of dual-wavelength X-ray sources. One model (Dual Wavelength=DW) can generate two distinct characteristic X-ray wavelengths from one rotating-anode target by using a double-banded target. The other is (DualSource=DS) a system that has two independent X-ray sources.



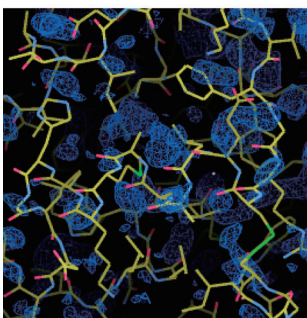
MAD



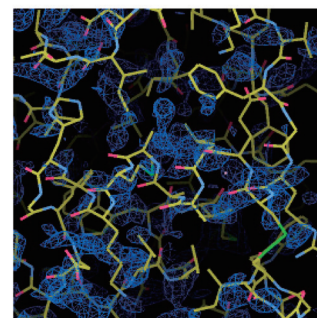
SIRAS (CuK $\alpha$ )



SIRAS (MoK $\alpha$ )



SAD (CuK $\alpha$ )



SAD (MoK $\alpha$ )

**Fig. 5.** Electron density maps.



**Fig. 6.** VariMax DW with RAPID II system.



Fig. 7. VariMax DW with Saturn system.



Fig. 8. R-Axis series.

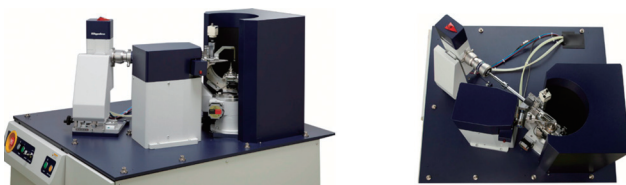


Fig. 9. DualSource RAPID II system.

The VariMax DW system has an X-ray generator and mirror device for two wavelengths and is capable of delivering two highly brilliant X-rays wavelengths to a sample. In the VariMax DW with RAPID II system, the separation of diffraction spots is superior because the distance from crystal to detector is 127 mm. Therefore, it is suitable not only for the crystals of small molecules but also for macromolecules and powder diffraction.



Fig. 10. DualSource CCD system.



Fig. 11. An attachment for elemental analysis: EElement ANalyzer.

The VariMax DW with Saturn system has a highly sensitive CCD detector. This DW system is available as an option for FR-X system, the world's highest intensity microfocus rotating anode X-ray generator, and the MicroMax007, the world's most popular microfocus rotating anode generator. In addition, it is possible to substitute the R-Axis IV or VII (HTC) for the Saturn CCD for labs that prefer imaging plate technology.

On the other hand, a DS system has two independent sealed-tube generators. It is easy to measure with two wavelengths because it is not necessary to change tubes to get X-rays of another wavelength. The DualSource RAPID II system has a Cu MicroMax003 microfocus generator and a Mo 3 kW sealed-tube generator for the X-ray resources, and a curved image plate for the detector. The DualSource CCD system has two MicroMax003 generators and a CCD detector. Each particular system has its own set of strengths and the choice is dependent on the type of research being performed.

#### 4.2. An attachment for elemental analysis: EElement ANalyzer

Our new product—the EElement ANalyzer is a state-of-the-art attachment that allows us to obtain qualitative information on elements in a single crystal at the same time as X-ray diffraction data collection for a single crystal structural analysis. By measuring the X-ray fluorescence spectrum emitted during X-ray diffraction experiments with the EElement ANalyzer, it becomes possible to perform elemental analysis on a single grain of crystal, something that is considered to be difficult to do from the point of view of sample volume required for a measurement. An element having an atomic number higher than that of phosphorous can be identified with monochromated  $MoK\alpha$  radiation.

The ELeMent ANalyzer is designed to be able to be used in combination with the R-AXIS RAPID II system as well as the Saturn CCD system, so that there is no need to modify an existing system. In addition, the small and light body enable to be installed on other crystallography systems. A silicon drift detector (SDD), which requires no liquid nitrogen for cooling, is used as the detector of the ELeMent ANalyzer.

The ELeMent ANalyzer can be used not only for selection of isomorphous heavy-atom derivatives in protein structure determination, but also for confirmation the presence of central metal(s) in a

mononuclear or polynuclear complex or solvent in a crystal for small molecule X-ray crystallography. There is a broad range of possible applications of the ELeMent ANalyzer in the many fields of science.

### References

- (1) T. L. Blundell and L. N. Johnson: *Protein Crystallography*, Academic Press, London, (1976), 183–239.
- (2) K. Cowtan: *Acta Crystallogr. D.*, **64** (2008), 83–89.
- (3) Collaborative Computational Project, Number 4, *Acta Crystallogr. D.*, **50** (1994), 760–776.